Origin of ringlike angular distributions observed in rainbow channeling in ultrathin crystals

M. Motapothula,[1] S. Petrović,[2] N. Nešković,[2] Z. Y. Dang,[1] M. B. H. Breese,[1,3,*] M. A. Rana,[4] and A. Osman[5]

[1]*Center for Ion Beam Applications, Physics Department, National University of Singapore, Lower Kent Ridge Road, Singapore 117542, Singapore*

[2]*Laboratory of Physics, Vinča Institute of Nuclear Sciences, University of Belgrade, P.O. Box 522, 11001 Belgrade, Serbia*

[3]*Singapore Synchrotron Light Source (SSLS), National University of Singapore, 5 Research Link, Singapore 117603, Singapore*

[4]*Physics Division, Directorate of Science, PINSTECH, P.O. Nilore, Islamabad, Pakistan*

[5]*National Centre for Physics (NCP), Shahdura Valley Road, Islamabad, Pakistan*

(Received 29 May 2012; revised manuscript received 22 August 2012; published 26 November 2012)

Using the theory of crystal rainbows, we prove that the well-known doughnut patterns observed in ion channeling in thin crystal membranes are manifestations of the rainbow effect. This is done by a detailed morphological study of the high-resolution experimental angular distributions of 2 MeV protons channeled in a 55-nm-thick (001) silicon crystal tilted away from the [001] direction. The inner side of the doughnut is the dark side of the rainbow, analogous to the Alexander's dark band, occurring between the primary and secondary meteorological rainbows.

DOI: 10.1103/PhysRevB.86.205426 PACS number(s): 61.85.+p

I. INTRODUCTION

Axial ion channeling is the process of ion motion through axial crystal channels in which the angle of the ion's velocity vector relative to the channel axis remains small.[1] Analogously, planar ion channeling is the process of ion propagation through planar crystal channels. When the incident ion beam is tilted away from a major crystallographic direction, the angular distribution of channeled ions exhibits a ringlike shape. This effect, named the doughnut effect, has been well studied by many researchers.[2–4] Nevertheless, its origin has not yet been revealed.

Here, we present a detailed morphological analysis of a set of high-resolution ion channeling observations conducted with a proton beam with energy of 2 MeV and an ultrathin (001) silicon crystal. The thickness of the crystal was 55 nm, and it was tilted away from the [001] direction. Our objective was to characterize the doughnut effect and answer the question of its origin. The analysis was performed using the theory of crystal rainbows.[5,6]

II. CRYSTAL RAINBOWS

It was shown theoretically that a rainbow occurred during ion transmission through an axial channel of a very thin crystal.[5] The model was purely classical, and the effect was explained by the complex contributions of the crystal's atomic strings to the ion differential transmission cross section. Namely, this variable includes the terms describing the contributions of individual atomic strings as well as the terms describing the joint contributions of pairs of atomic strings. This is a manifestation of the fact that the crystal is more than a simple sum of its atomic strings. Hence, the effect is a *gestalt* or *synergistic* effect. As a result, the obtained angular distribution of transmitted ions can be complex and its geometrical interpretation difficult or even impossible. It was further demonstrated that the effect, named the crystal rainbow effect, could be modeled accurately using catastrophe theory.[7–9] Therefore, one can say that it is a *catastrophic* effect too.

The crystal rainbow effect was observed experimentally by Krause *et al.*[10,11] In the former measurement, the projectiles were 7 MeV protons, and they were transmitted through axial channels of either a 140-nm-thick (001) or a 198-nm-thick (011) silicon crystal in the aligned case. The corresponding values of reduced crystal thickness were 0.23 and 0.24, respectively. This variable is defined as

$$\Lambda = f_h \frac{L}{v_0}, \tag{1}$$

where L is the crystal thickness, v_0 is the magnitude of initial ion velocity vector, and f_h is the frequency of ion motion close to the channel axis.[11] The fact that the two chosen values of Λ were below 0.25 meant that the crystals were very thin.[6,12] The results were analyzed and explained by the model of crystal rainbows[5] and the Lindhard's proton–atom interaction potential.[13]

In the latter measurement of Krause *et al.*,[11] the projectiles were 2–9 MeV protons and 6–30 MeV C^{4+}, C^{5+}, and C^{6+} ions, and they were transmitted through axial channels of either a 179-nm-thick or a 190-nm-thick (001) silicon crystal in the aligned case. The corresponding values of Λ were between 0.25 and 1. The obtained results were interpreted using the LAROSE three-dimensional computer simulation code[14,15] and the Molière's ion–atom interaction potential.[16] All the maxima appearing in the experimental angular distributions of transmitted ions, which were attributed to the zero-degree focusing effect and rainbow effect, coincided with the corresponding theoretical maxima.

In such experiments,[10,11] the angular resolution of transmitted patterns is determined by the energy, energy spread, and divergence or convergence angle of the incident ion beam, the diameter of the beam spot at the crystal surface, the crystal quality, thickness, and alignment, the detector characteristics and its distance from the crystal, and the effect of collisions between the ions and crystal's electrons. In those measurements, the resolution was not sufficiently high to observe the details of angular distributions of transmitted ions.

III. THEORY OF CRYSTAL RAINBOWS

In order to describe ion channeling in axial channels of crystals that were not necessarily very thin, the model given in Ref. 5 was generalized and formulated into the theory of crystal rainbows.[6] The theory enables one to generate the whole angular distribution of channeled ions, i.e., its component corresponding to the part of the channel in the vicinity of its axis, as well its component corresponding to the part of the channel in the vicinity of the atomic strings defining the channel. It has been demonstrated that the theory can be also applied to ion channeling in carbon nanotubes.[17] Let us now give a brief description of the part of the theory relevant for this study. We take that the z axis of the reference frame, being the longitudinal axis, coincides with the channel axis and that its origin lies in the entrance plane of the crystal. The x and y axes of the reference frame, being the transverse axes, are the vertical and horizontal axes, respectively. Let us introduce mapping

$$\theta_x = \theta_x(x_0, y_0, \Lambda, \varphi) \quad \text{and} \quad \theta_y = \theta_y(x_0, y_0, \Lambda, \varphi), \tag{2}$$

where x_0 and y_0 are the transverse components of the initial ion position vector, i.e., the components of its impact parameter vector, θ_x and θ_y are the components of the final ion channeling angle, i.e., the components of its transmission angle, and φ is the crystal tilt angle. It is the mapping of the impact parameter plane to the transmission angle plane. This mapping has proven to be highly nonlinear. In order to obtain θ_x and θ_y, the ion equations of motion must be solved. Since the ion channeling angle is small, i.e., it is always smaller than the axial channeling critical angle,[13] one can take that $\theta_x = v_x/v$ and $\theta_y = v_y/v$, where $v_x = v_x(x_0, y_0, \Lambda, \varphi)$ and $v_y = v_y(x_0, y_0, \Lambda, \varphi)$ are the transverse components of the final ion velocity vector, and $v = v(x_0, y_0, \Lambda, \varphi)$ is its magnitude.

We assume that the interaction of the ion and crystal can be treated classically. The interaction of the ion and a crystal's atom is described by the appropriate interaction potential. We apply either the binary collision approximation or the continuum approximation.[13] In the latter case, we obtain the ion–crystal continuum interaction potential as the longitudinally averaged ion–atom interaction potential summed over the atomic strings. One can include in this description the thermal vibrations of the crystal's atoms as well as the ion energy loss and dispersion of its channeling angle, caused by its collisions with the crystal's electrons.

Since the components of the ion channeling angle remain small during the whole transmission process, the ion differential transmission cross section is

$$\sigma(x_0, y_0, \Lambda, \varphi) = \frac{1}{|J_\theta(x_0, y_0, \Lambda, \varphi)|}, \tag{3}$$

where

$$J_\theta(x_0, y_0, \Lambda, \varphi) = \partial_{x_0}\theta_x \partial_{y_0}\theta_y - \partial_{y_0}\theta_x \partial_{x_0}\theta_y \tag{4}$$

is the Jacobian of functions $\theta_x(x_0, y_0, \Lambda, \varphi)$ and $\theta_y(x_0, y_0, \Lambda, \varphi)$. Hence, equation

$$J_\theta(x_0, y_0, \Lambda, \varphi) = 0 \tag{5}$$

gives the rainbow lines in the impact parameter plane. The images of these lines determined by functions $\theta_x(x_0, y_0, \Lambda, \varphi)$ and $\theta_y(x_0, y_0, \Lambda, \varphi)$ are the rainbow lines in the transmission angle plane. These lines separate the bright and dark regions in the transmission angle plane.

Nešković *et al.*[18] performed a theoretical study of the angular distributions and rainbow patterns of 10 MeV protons transmitted through a tilted 121-nm-thick (111) silicon crystal. The corresponding value of Λ was 0.15. It was found that the crystal rainbow effect evolved into the doughnut effect for larger values of φ.[2–4] A similar theoretical analysis, with the same conclusion about the connection of the rainbow and doughnut patterns, was performed with 10 MeV protons transmitted through axial channels of a tilted 100-nm-thick (011) silicon crystal.[19] The value of Λ in question was 0.11. However, until very recently, it had not been possible to measure the angular distributions for such small values of Λ.

IV. RESULTS AND DISCUSSION

We recently reported a series of high-resolution ion channeling measurements[20–22] using a 2 MeV proton beam focused to a small size spot with a diameter of about 1 μm on the surface of an ultrathin (001) silicon crystal. The objective was to measure the doughnut effect and reveal its origin. The crystal thickness was 55 nm, and it was tilted away from the [001], [011], and [111] directions. For protons of this energy propagating along the [001] direction, $\Lambda = 0.12$. The crystal was fabricated using the buried SiO_2 layer in a silicon-on-insulator wafer as a stop for KOH etching through a back-side opening in a protective polymer layer, producing a thin crystal surface area of about 0.5 mm^2 and with a roughness of about 0.4 nm.[20] The obtained results were reproduced using the FLUX three-dimensional computer simulation code[23,24] and the Ziegler–Biersack–Littmark (ZBL) proton–atom interaction potential.[25] The code is based on the binary collision approximation and takes into account the thermal vibrations of the crystal's atoms and the collisions between protons and the crystal's electrons.

As it has been said, the subject of this study is a detailed morphological analysis of a set of 2 MeV proton channeling measurements with such a crystal membrane using the theory of crystal rainbows. The initial proton beam propagates along the z axis. The atomic strings defining the channel intersect lines $y = x$ and $y = -x$. The crystal is tilted about the $-x$ axis by an angle in the range between $\varphi = 0.00$ and 0.15 degrees, equal to 43% of the axial channeling critical angle.[21]

The ZBL proton–crystal continuum interaction potential[25] in the case under consideration is shown in Fig. 1. The thermal vibrations of the crystal's atoms are taken into account. The values of continuum interaction potential have been calculated for the distances from the atomic strings defining the channel larger than the screening radius of the crystal's atoms. The figure clearly shows the potential well in which the channeled protons move, with its four steep walls, corresponding to the atomic strings defining the channel, and its two out of four shoulders, along the lines parallel to the horizontal axis connecting two upper and two lower atomic strings. For fixed values of Λ and φ, the details of this potential well determine the details of mapping of the impact parameter plane to the transmission angle plane, given by Eq. (2). However, it will be shown here later that the mappings for a fixed value of Λ and

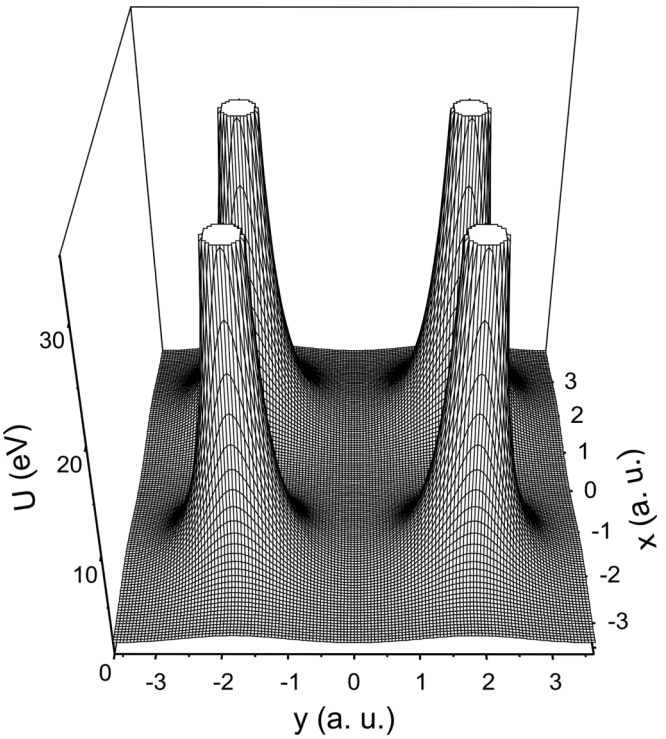

FIG. 1. The ZBL proton–crystal continuum interaction potential for 2 MeV protons moving along the [001] direction in a silicon crystal.

different values of φ can be qualitatively different from each other.

Figure 2 shows the angular distribution of 2 MeV protons transmitted through a 55-nm-thick (001) silicon crystal for $\varphi = 0.00$ degrees generated using the FLUX computer code[23,24] and

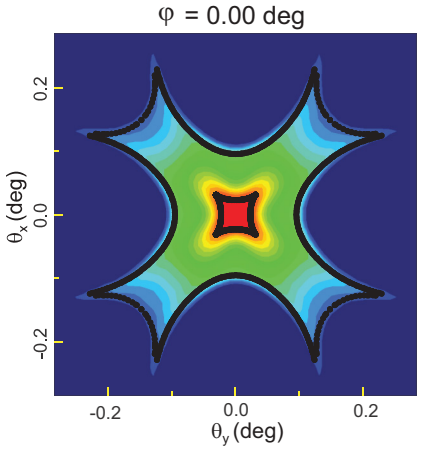

FIG. 2. (Color online) The theoretical angular distribution of 2 MeV protons transmitted through a 55-nm-thick (001) silicon crystal for $\varphi = 0.0$ degrees. The area in which the yield of transmitted protons is between 0% and 0.5% is designated by the dark blue color, the areas in which the yields are between 0.5% and 76.7% are designated by the varying tones of blue, green, yellow, and red colors, and the area in which the yield is between 76.7% and 100% is indicated by the dark red color. The black lines are the rainbow lines in the tranmission angle plane.

the ZBL proton–atom interaction potential.[25] The distribution is maximal at the origin, corresponding to the nondeflected beam, and has a fourfold rotational symmetry, resulting from the symmetrical arrangement of the atomic strings defining the channel.

This figure also shows the corresponding rainbow pattern in the transmission angle plane, obtained using the theory of crystal rainbows and the ZBL proton–crystal continuum interaction potential[25] with the thermal vibrations of the crystal's atoms included and the collisions between protons and the crystal's electrons neglected. We have found that contribution of the latter effect to the angular distributions of transmitted protons is minor. One clearly sees that the pattern fully determines the angular distribution in that it resembles the "skeleton" of the distribution. The pattern contains a line in the central region of the transmission angle plane composed of four equivalent parts that join to make four cusps directed toward the atomic strings defining the channel. It also contains four equivalent longer and four equivalent shorter lines in the peripheral region of the transmission angle plane that almost join to make eight cusps directed between the atomic strings defining the channel. The rainbow line in the impact parameter plane corresponding to each of these lines terminates in the vicinity of an atomic string, at the screening radius of the crystal's atoms, before joining the neighboring line. Beyond this limit, the continuum approximation is no longer valid—it cannot be used to determine the proper shape of the pattern in that region.

It has been found that the inner side of the central part of this rainbow pattern is the bright side of the rainbow and that its outer side is the dark side of the rainbow. The same is true for the peripheral part of the pattern.

Figure 3 gives a sequence of experimental angular distributions of 2 MeV protons transmitted through a 55-nm-thick (001) silicon crystal obtained by tilting the crystal away from the [001] direction. The included values of φ are 0.00, 0.05, 0.06, 0.07, 0.09, and 0.15 degrees. The distributions were recorded by photographing a highly sensitive aluminum-coated YAG scintilator screen placed 70 cm downstream of the crystal. The proton beam current was about 10 pA, the beam convergence angle was about 0.01 degrees, and the camera exposure time was 0.8 s. For $\varphi = 0.00$ degrees, the distribution is very similar to that in Fig. 2. As φ increases, it changes gradually from a squarelike to a ringlike distribution, appearing for $\varphi = 0.09$ degrees and being finally formed for $\varphi = 0.15$ degrees. For this value of φ, the yield of transmitted protons is maximal at the origin, decreases along the ring, extending along the θ_y axis, and exhibits eight cusps on the outer edge of the ring. This is the doughnut effect.[2–4,18,19] It should be noted that neither the squarelike distributions preceding the ringlike ones nor the cusps on their outer edges were observed with the thicker crystals.[2–4]

This figure also gives the corresponding rainbow patterns, calculated in the same way as that in Fig. 2. Again, one can clearly see that the patterns fully determine the corresponding angular distributions. The central part of the pattern, being a cusped square for $\varphi = 0.00$ degrees, changes to the cusped quasirectangles for $\varphi = 0.05$ and 0.06 degrees, to a cusped transition form for $\varphi = 0.07$ degrees, to a quasiellipse for $\varphi = 0.09$ degrees, and to a circle for $\varphi = 0.15$ degrees. On the other hand, the peripheral part of the pattern does not change

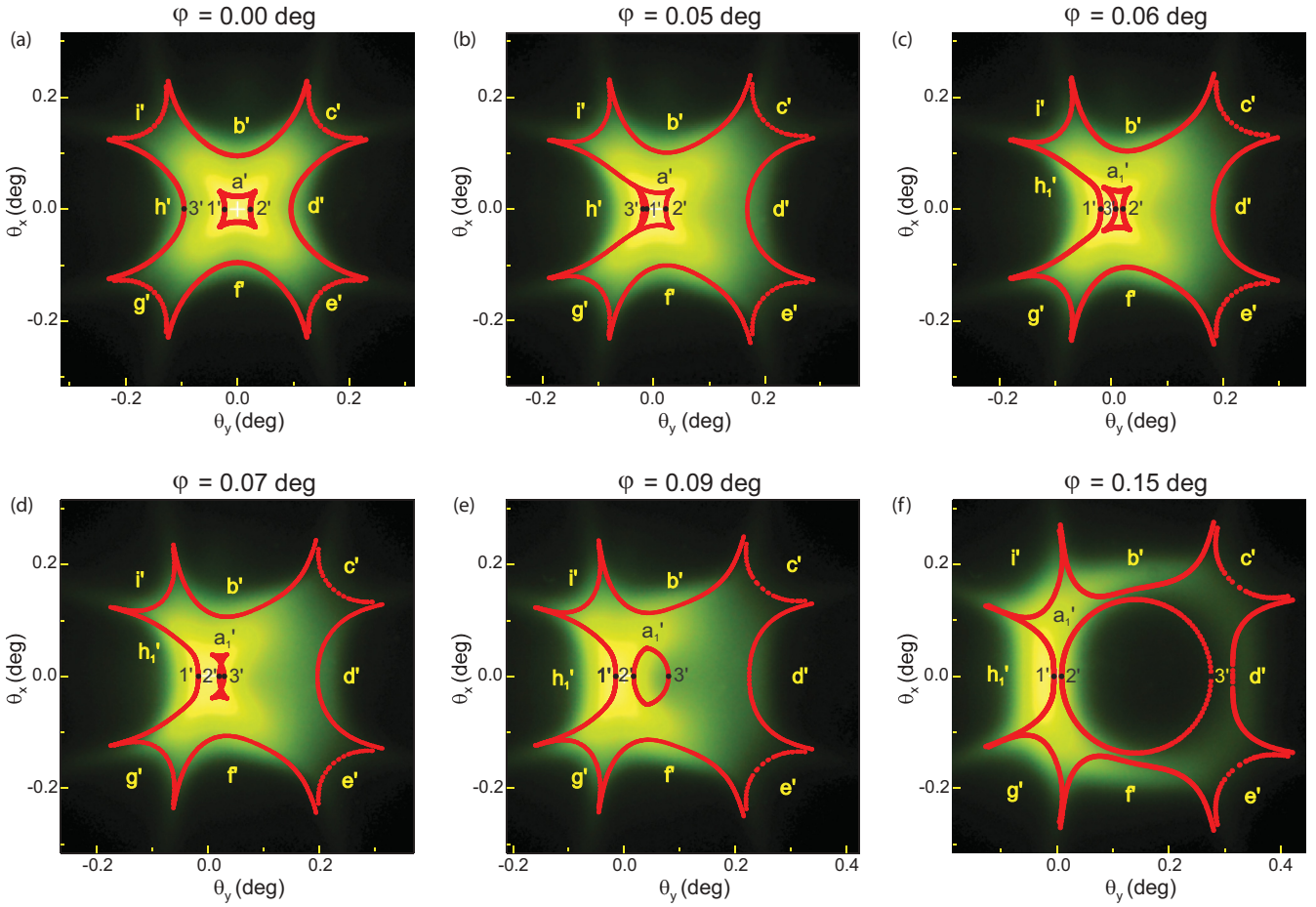

FIG. 3. (Color online) The experimental angular distributions of 2 MeV protons transmitted through a 55-nm-thick (001) silicon crystal for (a) $\varphi = 0.00$ degrees, (b) $\varphi = 0.05$ degrees, (c) $\varphi = 0.06$ degrees, (d) $\varphi = 0.07$ degrees, (e) $\varphi = 0.09$ degrees, and (f) $\varphi = 0.15$ degrees. The red lines are the rainbow lines in the tranmission angle plane.

much with φ. For the final value of φ, it contains three pairs of equivalent lines and two additional lines that almost join to make eight cusps.

Analysis has shown that the inner side of the central part of the rainbow pattern for $\varphi = 0.00$, 0.05, and 0.06 degrees is the bright side of the rainbow and that its outer side is the dark side of the rainbow. For $\varphi = 0.07$, 0.09, and 0.15 degrees, the situation is opposite. The inner side of the peripheral part of the pattern is the bright side of the rainbow, and its outer side is the dark side of the rainbow for all values of φ.

We now analyze the rainbow patterns in the impact parameter plane corresponding to the rainbow patterns shown in Fig. 3. Figure 4(a) gives the rainbow pattern in the impact parameter plane for $\varphi = 0.00$ degrees. It contains a line around the channel axis, designated as a, the image of which in the transmission angle plane is line a' in Fig. 3(a). The crossings of this line with the y axis are designated as 1 and 2, and their images as $1'$ and $2'$, respectively. This pattern also contains eight lines around each atomic string defining the channel, designated as b-i, the images of which in the transmission angle plane are lines b'-i' in Fig. 3(a), respectively. The crossing of line h with the line parallel to the y axis connecting the two upper atomic strings defining the channel is designated as 3 and its image as $3'$.

A detailed analysis of the evolution of this rainbow pattern in the impact parameter plane has shown that as φ increases, the lines it contains begin to "interact" with each other. In particular, lines a and h "attract" each other. For φ between 0.05 and 0.06 degrees, these lines join dividing line a into its right and left parts and line h into its upper, lower, and left parts. As a result, instead of line a, one obtains line a_1, being composed of the left part of line a and left part of line h, and line h_1, being composed of the right part of line a and upper and lower parts of line h. This is seen in Fig. 4(c), which gives the rainbow pattern in the impact parameter plane for $\varphi = 0.06$ degrees. It is evident that line a_1 connects the neighboring channels and line h_1 connects the neighboring atomic strings along the x axis. The rainbow patterns in the impact parameter plane for $\varphi =$ 0.07, 0.09, and 0.15 degrees are shown in Fig. 4(c). For $\varphi =$ 0.15 degrees, line a_1 is close and almost parallel to the x axis.

We now return to the rainbow patterns in Fig. 3, which are the images of the rainbow patterns in Fig. 4. For $\varphi = 0.00$ and 0.05 degrees, line a' contains points $1'$ and $2'$, and line h' contains point $3'$. However, for $\varphi = 0.06$ degrees, i.e., after the joining of lines a' and h', point $1'$ belongs to line h_1', and point $3'$ belongs to line a_1'. Point $3'$ is closer to the origin than point $2'$. The region between these two points, being on the right side of point $3'$ and the left side of point $2'$, is the

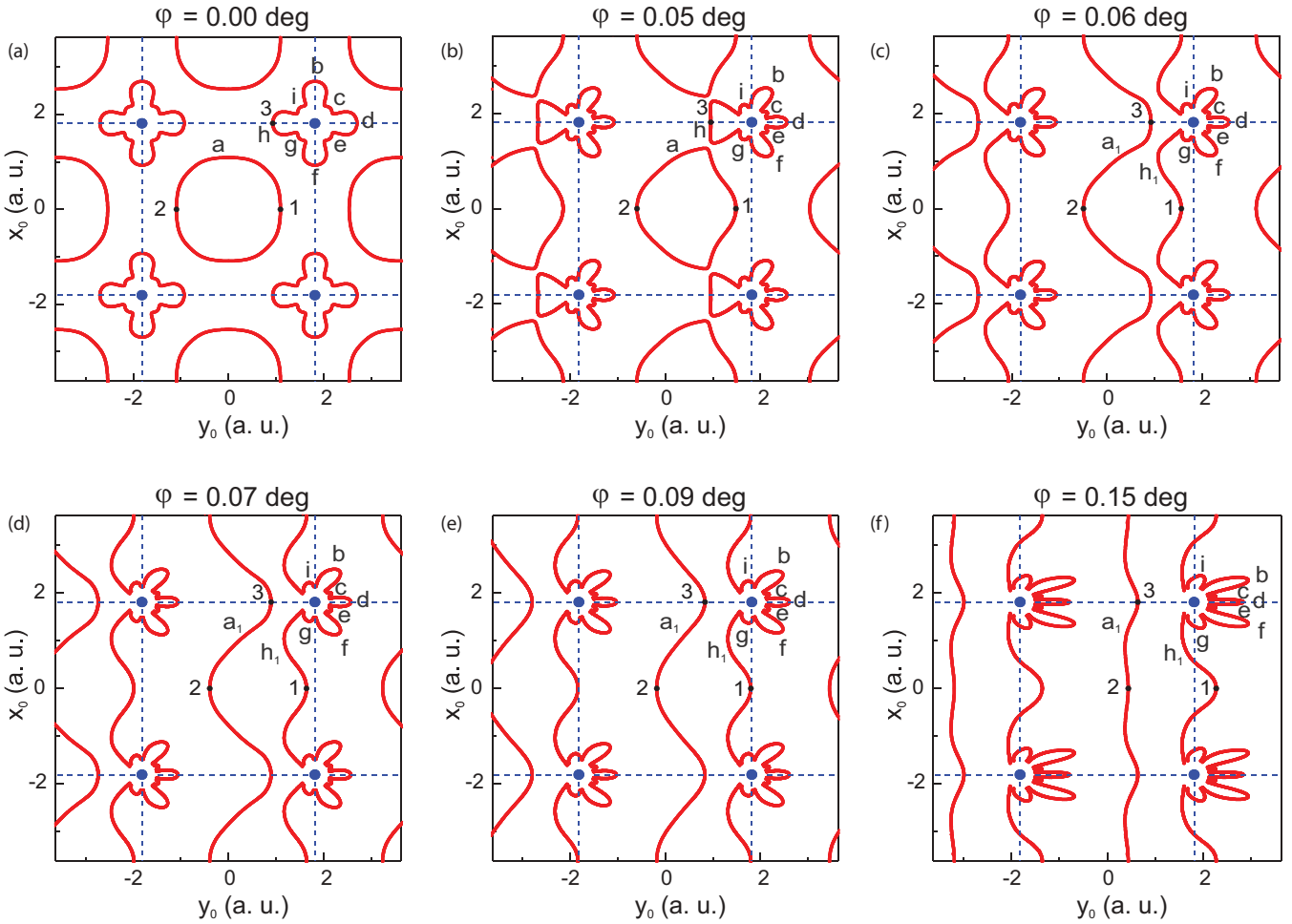

FIG. 4. (Color online) The rainbow patterns in the impact parameter plane for 2 MeV protons transmitted through a 55-nm-thick (001) silicon crystal for (a) $\varphi = 0.00$ degrees, (b) $\varphi = 0.05$ degrees, (c) $\varphi = 0.06$ degrees, (d) $\varphi = 0.07$ degrees, (e) $\varphi = 0.09$ degrees, and (f) $\varphi = 0.15$ degrees; 1 a.u. (atomic unit) = 0.052917 nm. The blue solid circles represent the atomic strings defining the channel.

bright side of the rainbow. As φ increases further, points $2'$ and $3'$ move toward each other, join, and move away from each other. This is seen in Figs. 3(d) and 3(e). For $\varphi = 0.07$, 0.09, and 0.15 degrees, point $3'$ is farther from the origin than point $2'$. Now, the region between these two points, being on the right side of point $2'$ and the left side of point $3'$, is the dark side of the rainbow. This region is an analogue of the Alexander's dark band, occurring between the primary and secondary meteorological rainbows.[26]

V. CONCLUSIONS

We have proven in this detailed morphological study of the experimental distributions of protons transmitted through an ultrathin silicon crystal that doughnuts are rainbows with tilted crystals. The study has been performed using the theory of crystal rainbows, which includes a precise analysis of the mapping of the impact parameter plane to the transmission angle plane. This mapping is described by the Jacobian of the components of proton transmission angle as functions of the components of its impact parameter vector. The lines in the impact parameter plane along which this variable is equal to zero are the rainbow lines in this plane. The rainbow lines in the transmission angle plane are the images of the ranbow lines in the impact parameter plane.

The results of our study clearly demonstrate that the theory of crystal rainbows is the proper theory of ion channeling in very thin crystals. It ensures excellent agreement between results of calculations and high-resolution ion channeling measurements with such crystals.

ACKNOWLEDGMENT

M.A.R wishes to thank I. R. Rahman, A. T. Fatami, N. M. Butt, Dr. Naaz, and Maria Nazeer for their computational support. S.P. and N.N. acknowledge the support to this work provided by the Ministry of Education, Science and Technological Development of Serbia through project "Physics and Chemistry with Ion Beams," No. III 45006.

*Corresponding author: phymbhb@nus.edu.sg

[1]D. S. Gemmell, Rev. Mod. Phys. **46**, 129 (1974).
[2]L. T. Chadderton, J. Appl. Crystallogr. **3**, 429 (1970).
[3]J. S. Rosner, W. M. Gibson, J. A. Golovchenko, A. N. Goland, and H. E. Wegner, Phys. Rev. B **18**, 1066 (1978).

[4]S. K. Andersen, O. Fich, H. Nielsen, H. E. Schiøtt, E. Uggerhøj, C. Vraast Thomsen, G. Charpak, G. Petersen, F. Sauli, J. P. Ponpon, and P. Siffert, Nucl. Phys. B **167**, 1 (1980).
[5]N. Nešković, Phys. Rev. B **33**, 6030 (1986).
[6]S. Petrović, L. Miletić, and N. Nešković, Phys. Rev. B **61**, 184 (2000).
[7]N. Nešković and B. Perović, Phys. Rev. Lett. **59**, 308 (1987).
[8]N. Nešković, G. Kapetanović, S. Petrović, and B. Perović, Phys. Lett. A **179**, 343 (1993).
[9]N. Nešković, S. Petrović, G. Kapetanović, B. Perović, and W. N. Lennard, Nucl. Instrum. Methods Phys. Res. B **93**, 249 (1994).
[10]H. F. Krause, S. Datz, P. F. Dittner, J. Gomez del Campo, P. D. Miller, C. D. Moak, N. Nešković, and P. L. Pepmiller, Phys. Rev. B **33**, 6036 (1986).
[11]H. F. Krause, J. H. Barrett, S. Datz, P. F. Dittner, N. L. Jones, J. Gomez del Campo, and C. R. Vane, Phys. Rev. A **49**, 283 (1994).
[12]N. Nešković, S. Petrović, and L. Živković, Eur. Phys. J. B **18**, 553 (2000).
[13]J. Lindhard, Mat. Fys. Medd. K. Dan. Vidensk. Selsk. **34**, 1 (1965).
[14]J. H. Barrett, Phys. Rev. B **3**, 1527 (1971).
[15]J. H. Barrett, Nucl. Instrum. Methods Phys. Res. B **44**, 367 (1990).
[16]G. Molière, Z. Naturforsch. A **2**, 133 (1947).
[17]S. Petrović, D. Borka, and N. Nešković, Eur. Phys. J. B **44**, 41 (2005).
[18]N. Nešković, S. Petrović, D. Borka, and S. Kossionides, Phys. Lett. A **304**, 114 (2002).
[19]D. Borka, S. Petrović, and N. Nešković, J. Electron Spectrosc. **129**, 183 (2003).
[20]Z. Y. Dang, M. Motapothula, Y. S. Ow, T. Venkatesan, M. B. H. Breese, M. A. Rana, and A. Osman, Appl. Phys. Lett. **99**, 223105 (2011).
[21]M. Motapothula, Z. Y. Dang, T. Venkatesan, M. B. H. Breese, M. A. Rana, and A. Osman, Nucl. Instrum. Methods Phys. Res. B **283**, 29 (2012).
[22]M. Motapothula, Z. Y. Dang, T. Venkatesan, M. B. H. Breese, M. A. Rana, and A. Osman, Phys. Rev. Lett. **108**, 195502 (2012).
[23]P. J. M. Smulders and D. O. Boerma, Nucl. Instrum. Methods Phys. Res. B **29**, 471 (1987).
[24]P. J. M. Smulders, D. O. Boerma, and M. Shaanan, Nucl. Instrum. Methods Phys. Res. B **45**, 450 (1990).
[25]J. F. Ziegler, J. P. Biersack, and U. Littmark, *The Stopping and Range of Ions in Solids* (Pergamon Press, New York, 1985).
[26]H. M. Nussenzveig, J. Math. Phys. **10**, 82 (1969); **10**, 125 (1969); Sci. Am. **236**, 116 (1977).